Original Article

Ruta graveolens methanol extract, fungal-mediated biosynthesized silver nanoparticles, and their combinations inhibit pathogenic bacteria

Nedaa Fawzi Husein[1], Amjad Asri Al-Tarawneh[2], Shahed Rashad Al-Rawashdeh[3], Khaled Khleifat[3*], Muhamad Al-Limoun[4], Ibrahim Alfarrayeh[5], Ahmad Eyal Awwad[4], Ahmad Za'al AlSarayreh[4], Yaseen Taha Al-Qaisi[4]

[1]Department of Allied Medical Sciences, Zarqa College, Al-Balqa Applied University, Zarqa 13110, Jordan. [2]Prince Faisal Center for Dead Sea, Environmental and Energy Research, Mutah University, Mutah, Karak, Jordan. [3]Department of Medical Laboratory Sciences, Faculty of Allied Medical Sciences, Mutah University, Al-Karak, Jordan. [4]Department of Biological Sciences, Faculty of Science, Mutah University, Al-Karak, Jordan. [5]Department of Applied Biology, Faculty of Science, Tafila Technical University, 66110 Tafila, Jordan.

Correspondence: Khaled Khleifat, Department of Medical Laboratory Sciences, Faculty of Allied Medical Sciences, Mutah University, Al-Karak, Jordan. alkhkha@hotmail.com

ABSTRACT

Silver nanoparticles (AgNPs) have been shown to be able to inhibit bacterial growth while presenting a negligible threat to the development of bacterial resistance and the toxicity of conventional silver compounds to human cells. Various concentrations of *R. graveolens* MetOH extract, both by itself and in combination with AgNPs made by *Aspergillus flavus*, were tested against several clinical isolates of Gram-positive and Gram-negative bacteria in the current study using disc diffusion methods and minimal inhibitory concentrations (MIC). *Klebsiella pneumoniae*, *Escherichia coli*, *Enterobacter cloacae*, *Pseudomonas aeruginosa*, *Shigella* sp., *Staphylococcus aureus*, and *Staphylococcus epidermidis* were the clinical bacteria types used in this research. Utilizing LC-MS, the chemical profile of the methanol extract of *R. graveolens* was investigated. AgNPs were initially identified by the development of a dark brown tint, UV-Vis spectroscopy, images of TEM, and the ATR-IR analysis. AgNPs and *R. graveolens* MetOH extract demonstrated synergistic effects on all of the examined microbes. Despite having the highest sensitivity to both the AgNPs and the *R. graveolens* MetOH extract when used separately (with inhibition zones of 16 and 19 mm, respectively), S. aureus has the lowest IFA values (0.10-0.13) when compared to the other bacterial strains, and no synergistic activity was shown. With a 1.25-fold rise in IFA, AgNPs and the *R. graveolens* MetOH extract had the strongest synergistic effect against S. epidermidis. By combining nanoparticles (NPs) with antibiotics or various types of medicinal plant extract, these results could be used to create and enhance novel antibacterial therapies as cutting-edge medications.

Keywords: Fungi, Nanoparticles, Antibacterial agents, Nanomedicine, *Ruta graveolens*

Introduction

Nanoparticle is a term, which usually includes the prefix "nano", which means its size is 10^{-6} of a millimeter. The second part of the word refers to the quality and origin of these molecules [1]. It could be three-dimensional particles, fibers with two outer dimensions, or plates with one outer dimension [2]. The study of the properties, structures, and knowledge of nanoparticles is the subject of nanoscience, one of the most significant fields of contemporary science. Additionally, how these nanoparticles might be used in all technological and scientific areas [3]. Nanotechnology is used almost everywhere, including in many academic areas like engineering, pharmacy, and medicine [4]. As a result, it is regarded as one of the more contemporary and active areas of the sciences.

Based on numerous scientific study findings in this area, the industry underwent a significant transformation starting with the

Access this article online	
Website: www.japer.in	**E-ISSN:** 2249-3379

How to cite this article: Husein NF, Al-Tarawneh AA, Al-Rawashdeh SR, Khleifat Kh, Al-Limoun M, Alfarrayeh I, et al. *Ruta graveolens* methanol extract, fungal-mediated biosynthesized silver nanoparticles, and their combinations inhibit pathogenic bacteria. J Adv Pharm Educ Res. 2023;13(2):43-52. https://doi.org/10.51847/H8saGkIapx

This is an open access journal, and articles are distributed under the terms of the Creative Commons Attribution-Non Commercial-ShareAlike 4.0 License, which allows others to remix, tweak, and build upon the work non-commercially, as long as appropriate credit is given and the new creations are licensed under the identical terms.

production of raw materials or using building blocks whose end products are at the nanoscale [1]. However, according to Calderón-Jiménez, Johnson, *et al*. (2017), nanoparticles (NPs) are groups of atoms that comprise at least one of the three outer dimensions and range in size from 1 to 100 nanometers [2]. Usually, when compared to their larger peers, nanoparticles display a variety of distinct physical or chemical properties and come in various sizes [5]. Numerous industries, including medicine, cosmetics, pharmaceuticals, green energy, the polymer industry, environmental treatment, water purification, and the production of some medical devices, may use the novel properties discovered at the nanoscale [6]. It is possible to create nanoparticles using physical, molecular, and biological processes. The chemical methods can produce nanoparticles in large amounts and quickly, but they frequently require the use of materials that are toxic and act as stabilizers and helpers at the same time. As a result, the byproducts produced by these methods are not ecologically friendly. While physical methods are fast because they don't require toxic chemicals to reduce the radioactive materials, they also have a low production capacity, require a lot of energy, and can contaminate organic solvents with nanoparticles of unintended sizes [7-9]. Biosynthesis through green nanotechnology, which uses biological (intracellular and extracellular) techniques using bacterial, fungal, and plant cells or their extracts, is a safe synthetic method because it is inexpensive, safe, and uses non-toxic chemicals without the creation of any hazardous byproducts [10]. Metal nanoparticles display distinct and novel physical and chemical properties in comparison to their macro-scale counterparts due to their size and large surface area [11]. One of the most common metal nanoparticles, silver nanoparticles (AgNPs), has effectively made its way into a variety of consumer goods, including soaps, textiles, and plastics [12]. They are also regarded as highly effective antimicrobial agents with broad-spectrum action against a variety of pathogenic bacteria and fungi. The biosynthesis, characterization, and assessment of AgNPs' antibacterial properties were the main objectives of this research. Therefore, using disc diffusion techniques, these biosynthesized nanoparticles were examined as an antibacterial agent against different Gram-negative and Gram-positive bacteria both with and without the addition of a plant extract of *Ruta graveolens*.

Materials and Methods

Fungal strain

Dr. Amjad Al-Tarawneh of the Dead Sea Institute for Water and Energy at Mutah University in Jordan isolated this fungus from the storage facilities of the Supplies Department. Aspergillus flavus was the only species that could be determined about the fungus strain through ITS sequencing (MACROGEN, Korea). In order to register the sequence in the NCBI database and acquire the accession number MG973280.1, a sequence similarity analysis with the NCBI database was first conducted [13].

Biosynthesis of silver nanoparticles (AgNPs)

For the synthesis of silver nanoparticles, the technique described by Jaidev and Narasimha (2010) was used, with a few small modifications that will be mentioned as necessary. In a nutshell, the fungal isolate was grown for 24 hours in a liquid culture medium with a pH of 7 under aerobic circumstances by inoculating the medium (100 mL) with 2.0×10^6 spores at 33 and 150 rpm, respectively. Following the extraction of fungal biomass using Whatmann No. 1 filter paper, the material was carefully cleaned with sterile and distilled water. Ten grams of wet biomass were added to 100 milliliters of sterile deionized water, which was then incubated for 48 hours at 33 °C, pH 7.0, and 150 rpm. The fungal biomass was then separated from the suspension using filtration paper to produce the fungal filtrate (Whitman No. 1). AgNO3 was added to the fungal filtrate (100 milliliters) at a concentration of 1 mM to complete the biosynthesis process. The filtrate was then kept for a further 24 hours in the dark at a temperature of 33 degrees and a shaking rate of 150 rpm, or longer if necessary. The pellet of silver nanoparticles was then vacuum-desiccated after recovery (VWR 1410 Vacuum Oven, USA). The biosynthetic silver nanoparticles (AgNPs) were first characterized using scanning ultraviolet-visible (UV/VIS) radiation in the 280–800 nm wavelength range. TEM images of the size, distribution, and shape of the created AgNPs were taken. The test flask was treated in the same manner but did not contain any AgNO3. Using a Bruker Alpha FTIR spectrometer, functional groups important for AgNP stability, such as proteins, have been identified (Bruker Optics GmbH, Ettlingen, Germany) [13].

Preparation of bacterial suspension

The growth medium was created in accordance with Laboratory Standards Institute guidelines [14]. A single bacterial colony was chosen and grown overnight at 37 °C in sterile 5 ml (NB) nutrient broth. Using sterile NB broth, the rate of bacterial growth was fixed at 0.5 McFarland Standard, and the final absorbance was 0.1 at 600 nm. The Al Bashir Hospital provided the clinical bacterial samples (Amman, Jordan). Escherichia coli, Klebsiella pneumonia, E. cloacae, Shigella sp., Pseudomonas aeruginosa, Staphylococcus aureus, and Staphylococcus epidermidis were among the bacterial types examined. Using BIOMÉRIEUX VITEK® 2, all isolates' IDs were verified [15-17].

Preparing the extracts of R. graveolens

R. graveolens' fresh aerial parts were cleaned, dried, and powdered in a mixer. 100 grams of the desiccated plant were soaked in 1000 ml of methanol (1:10 w/v) at room temperature for 72 hours with constant shaking. Following filtering, the extract was low-pressure, 45 °C-dried in a rotary evaporator. At -20 °C, the produced extract was stored. The following equation was used to determine the yield rate:

Yield % = (wt. of dry extract / wt. of dry parts before extraction) x 100%. Finally, the stock solution was made by dissolving 500 mg/mL of the dried crude extract by using 30% DMSO (dimethyl sulfoxide). A series of dilutions were prepared for obtaining concentrations of 2.5, 5, 7.5, and 10 mg/mL.

LC–MS analysis of R. graveolens composition

Liquid chromatography-mass spectrometry was used to examine the *R. graveolens* composition LC–MS). A 0.1 percent (v/v) formic acid in water was used as solvent A, and 0.1 percent (v/v) formic acid in acetonitrile was used as solvent B, for the following gradient: 5 percent B for 5 minutes, 5-100 percent B in 15 minutes, and 100 percent for 5 minutes. This HPLC separation was carried out at a flow rate of 0.5 ml/min. The Agilent Zorbax Eclipse XDB-C18 column (2.1 150 mm 3.5 um) was utilized. The oven temperature was 25 °C, and the sample injection volume was 1 l (18 mg/mL in methanol). Using a positive-ion mode Shimadzu LC-MS 8030 equipped with an electrospray ion mass spectrometer, the eluent was scanned from 100 to 1000 m/z with a secondary scan from 50 to 100 m/z MRM mode (ESI-MS). A 125 V fragment piece and a 65 V skimmer were used for the ESI. Using a flow rate of 10 L/min, a nebulizer pressure of 45, and a capillary temperature of 350 C, high-purity nitrogen (99.999%) was employed as the drying gas. Parallel applications of a formic acid blank at 0.1 percent were made. A sample was injected into the mass detector using the Shimadzu CBM-20A system controller, the LC-30AD pump, the SIL-30AC autosampler with cooler, and the CTO-30 column oven.

Antibacterial activities of R. graveolens MetOH extract and AgNPs solution

Diffusion assays were carried out in Mueller Hinton Agar containing Petri dishes. Ready-made 6-mm paper disc diffusion tests were performed for the *R. graveolens* MetOH extract [18]. Discs placed on the agar surface were impregnated with 2.5, 5, 7.5, and 10 mg/ml *R. graveolens* MetOH extract. For the AgNPs solution, discs placed on the agar surface were impregnated with different concentrations of 0.125, 0.25, 0.375, 0.5, 1, and 1.5 mg/ml. After 24 h, the potential zone of inhibition for AgNP doses and *R. graveolens* MetOH extract concentration against all bacterial samples were monitored and calculated.

MIC assays

MIC is the lowest concentration of the substance needed to kill bacteria. Dilutions were prepared from a DMSO- *R. graveolens* MetOH extracts stock solution with 500 mg/ml *R. graveolens* MetOH extract concentration to obtain 0.5, 1, 1.5, 2, 2.5, 5, 7.5, and 10 mg/ml *R. graveolens* MetOH extract concentration. For AgNPs solution, a series of volumes were made to obtain 0.025, 0.05, 0.075, 0.1, 0.125, 0.25, 0.375, 0.5, 1, and 1.5 mg/ml AgNPs concentration from a stock solution of 25 mg/ml AgNPs concentration. After 24 h, the zone of inhibition of each sample was monitored and calculated. Determination of synergy between AgNPs and *R. graveolens* MetOH extract.

Determination of synergy between AgNPs and R. graveolens MetOH extract

In the synergy experiments using disc diffusion, ready-made discs were used. Before determining the concentrations that were used in the synergistic experiments, 2.5, 5, 7.5, and 10 mg/ml *R. graveolens* MetOH extract and 0.125, 0.25, 0.375, 0.5, 1, and 1.5 mg/ml of AgNPs were used on each disc to be tested against seven bacterial species mentioned above. For studies on the synergy of combination between the two substances, each tested disc contained 2.5 mg/ml of *R. graveolens* MetOH extract, and 0.125, 0.25, 0.375, 0.5 mg/ml of AgNPs solution were used together [19, 20]. The synergistic effect was evaluated by using IFA unit increases [21].

$$IFA = B^2\text{-}A^2 / A^2 \quad (1)$$

Where A and B are the zones of inhibition (mm) produced by only *R. graveolens* MetOH extract or a combination of *R. graveolens* MetOH extract with AgNPs. When the inhibition value was zero, then the diameter of the disc was considered 6 mm for calculation purposes.

Results and Discussion

In this study, the potential for combining the *R. graveolens* MetOH extract with biologically produced silver nanoparticles by the isolated air-born fungus *Aspergillus flavus* was examined. The fungus filtrate's intense dark brown color first showed 24 hours after AgNO3 was added **(Figure 1)**. They were able to produce silver nanoparticles in vitro due to the extracellular release of several fungus enzymes and the ease with which they maintained their efficacy. Nanoparticles' TEM images show that they are spherical and range in size from 10 to 45 nm **(Figure 2)**. It has still not been possible to fully understand how fungi produce AgNP.

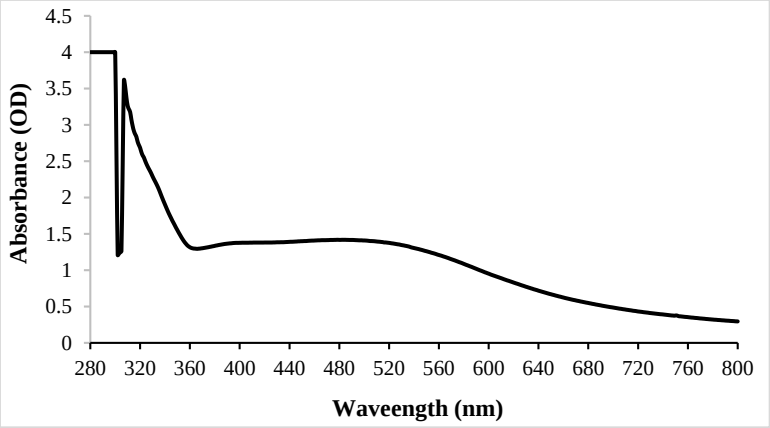

Figure 1. Formation of dark brown color and UV-Vis spectroscopy of the fungal filtrate that appeared after 24 h of the addition of $AgNO_3$.

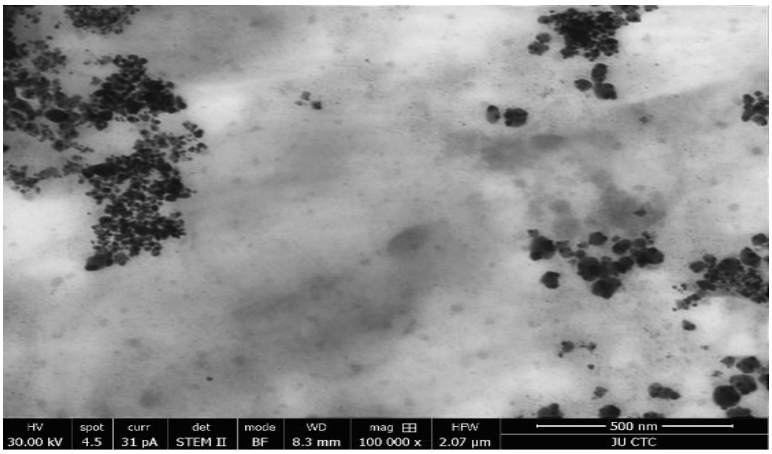

Figure 2. TEM micrograph of silver nanoparticles synthesized by the reaction of 1.0 mM silver nitrate with the fungal filtrate. Magnification 100,000x.

Analysis of the ATR-IR spectrum

The ATR-FTIR spectra, shown in **Figure 3**, showed significant peaks at 1011, 1375, 1437, 1516, 1623, and 2401 cm^{-1}, as well as a somewhat flat peak at about 3228 cm^{-1}. The big peak between 3228 cm-1 and 2827 cm^{-1} is caused by the vibrational resonant frequency of hydrogen-containing bonds such as C-H, O-H, and N-H. The COO- group is stretched in both a symmetrical and an asymmetrical manner, as evidenced by the significant absorption intensity values at the peaks at 1623, 1516, and 1081 cm^{-1}. The groups of amino and aminomethyl stretch of the protein are the sole stretch group peaks in the spectrum at 1375 cm^{-1}.

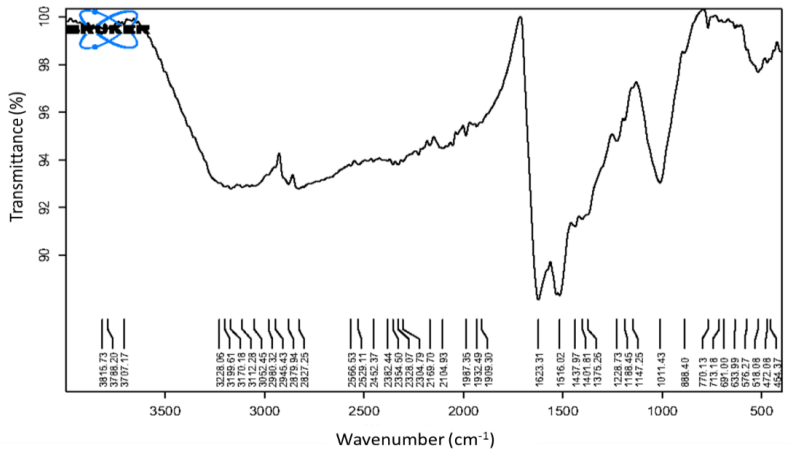

Figure 3. Silver nanoparticles made biologically were examined using ATR-IR.

Antibacterial effect of AgNPs and R. graveolens MetOH extract

The antibacterial activities were examined using the agar disc diffusion assay on Mueller-Hinton agar against the Gram-positive bacteria *Staphylococcus aureus* and *Staphylococcus epidermidis* as well as the Gram-negative bacteria *Escherichia coli, Klebsiella pneumonia, E. cloacae, Shigella sp*., and *Pseudomonas aeruginosa*. Each bacterial strain was dispersed evenly all over the surface of the agar after being adjusted to include 10^6 CFU/mL in the initial 100 µL inoculum. After that, AgNPs doses of 0.125, 0.25, 0.375, 0.5, 1, and 1.5 mg/mL were added to 6 mm diameter discs, and they were then incubated at 37°C for 24 hours. 100 mL of streptomycin solution was inoculated as a positive control using the same concentrations, and 100 µL of deionized water was used as a negative control. After a 24-hour incubation period, the inhibition zones were assessed. The assays were carried out three times.

The diameter of the inhibition zones created by AgNPs against different tested pathogenic bacteria was measured. The findings demonstrated that all concentrations of silver nanoparticles utilized had anti-bacterial effects for all bacteria tested and that these effects gradually increased with concentration. At a dosage of 0.125 mg/ml of AgNPs, *Escherichia coli*, *Klebsiella pneumonia*, *E. cloacae*, *Shigella* sp., *Pseudomonas aeruginosa*, *Staphylococcus aureus*, and *Staphylococcus epidermidis* were all inhibited, with inhibition zones measuring 7 to 9 mm. The inhibition zone of these bacteria ranged between 10 and 24 mm when using the higher AgNPs concentration (1.5 mg/ml).

Synergistic effects against K. pneumonia

Even though every dose of AgNPs that was tested has shown antibacterial activity against all bacterial strains **(Table 1)**, the lowest *R. graveolens* MetOH extract concentration utilized in synergistic tests was 2.5 mg/ml, and the AgNPs concentrations employed in combination with it were 0.125, 0.25, 0.375, and 0.5 mg/ml **(Table 1)**. IFA values of 0.36, 0.33, 0.31, and 0.14 were obtained when 0.125, 0.25, 0.375, and 0.5 mg/mL of AgNPs were combined with 2.5 mg/mL of *R. graveolens* MetOH extract, respectively. This combination exhibited a synergistic effect against K. pneumoniae and was more effective than either one alone **(Table 2)**. AgNPs or *R. graveolens* MetOH extract have quite distinct mechanisms of action, regardless of whether they are administered singly or in combination. The impact discovered in this investigation was the result of an interaction between AgNPs and MetOH extract.

Synergistic effects against E. coli

When AgNPs and *R. graveolens* MetOH extract were mixed, significant changes in the synergistic effects against *E. coli* were observed **(Tables 1-3)**. When different quantities of AgNPs (0.125, 0.25, 0.375, and 0.5 mg/ml) were combined with 2.5 mg/mL of *R. graveolens* MetOH extract, there were increases in IFA of 0.036, 0.33, 0.14, and 0.13, demonstrating the AgNPs' substantial synergy. The *E. coli* inhibitory zones were 9, 10, 11, 12, 13, and 14 mm when AgNPs were used alone and at concentrations of 0.125, 0.25, 0.375, 0.5, 1, and 1.5 mg/ml, respectively **(Table 1)**. In the presence of 2.5 mg/mL of *R. graveolens* MetOH extract, 0.25 mg/ml of AgNPs showed substantial effects (IFAs of 0.33) when used against *E. coli* **(Table 2)**.

Synergistic effects against E. cloacae

AgNPs had a substantial synergistic antibacterial effect against *E. cloacae* and ranged from 0.13 to 0.33 IFA when coupled with *R. graveolens* MetOH extract **(Tables 1-3)**. The concentration of 0.125 mg/mL AgNPs with 0.33 IFA produced the strongest meaningful effects.

Synergistic effects against S. aureus and S. epidermidis

All AgNPs and *R. graveolens* MetOH extract doses used in this study resulted in extraordinarily high sensitivity of the *Staphylococcus aureus* bacterial strain **(Tables 1-3)**. The IFA ranged from 0.10 to 0.13, and the synergistic result was slightly better when the two drugs were administered together than when they were used separately. The bacterial strain *S. epidermidis* exhibited the opposite outcomes when combined with 2.5 mg/ml of *R. graveolens* MetOH extract concentration, with IFA ranging from 0.19 at 0.125 mg/ml to 1.25 at 0.5 mg/ml AgNPs concentration **(Tables 1-3)**. Our *in vitro* research revealed, among other things, that *S. epidermidis* cells, unlike *S. aureus*, had established their sensitivity to all AgNP concentrations and MetOH extract from *R. graveolens*, both separately and in combination. The combined use of *R. graveolens* MetOH extract and data clearly showed a significant reduction in the required concentration of AgNPs.

Synergistic effects against Shigella sp.

Shigella species' inhibitory zones by various concentrations of AgNPs were revealed in a concentration-dependent way **(Table 1)**. When the same bacteria were exposed to an *R. graveolens* MetOH extract, the same behavior occurred to them, and the strength of the inhibition was influenced by the extract's concentration **(Table 2)**. When different AgNP doses were combined with 2.5 mg/ml of *R. graveolens* MetOH extract, the inhibition zones were increased as indicated by an increase in the fold area of inhibition (IFA), which ranged from 0.21 to 0.86 **(Table 3)**.

Synergistic effects against P. aeruginosa

P. aeruginosa was cytotoxic to every one of the AgNP doses used in the experiment, with inhibition zones between 7 and 10 mm. The inhibition zones ranged from 7 to 24 mm, and all of the

tested bacteria (*K. pneumonia, E. coli, E. cloacae, S. aureus, S. epidermidis, Shigella sp., and P. aeruginosa*) were susceptible to it to varied degrees **(Table 1)**. These variations in the sensitivity of gram-positive and gram-negative bacteria to nanoparticles may result from these differences in the cell surfaces of these bacteria [22, 23]. The activity of the AgNPs (such as antimicrobial efficacy) depends on their specific surface areas.

Investigators have looked into the naturally occurring AgNPs derived from fungi and their antibacterial properties. When AgNPs and *R. graveolens* MetOH extract were combined, the antimicrobial efficacy against *P. aeruginosa* was enhanced **(Table 3)**. The IFA of the synergistic findings were 0.25, 0.22, 0.72, and 0.21, respectively, for AgNP concentrations of 0.125, 0.25, 0.375, and 0.5 mg/ml **(Table 2)**.

However, the mixture of various AgNP doses and 2.5 mg/ml of *R. graveolens* MetOH extract showed acceptable susceptibility to *P. aeruginosa*, with considerable inhibitory zones between 19 and 22 mm.

Table 1. Antimicrobial activity of AgNPs and MeOH extract of *R. graveolens* (mg/ml) against the different tested bacterial species.

Conc. of AgNPs (mg/ml)	Inhibition zone (mm)						
	K. pneumoniae	*E. coli*	*E. clocae*	*S. aureus*	*S. epidermidis*	*Shigella* sp	*P. aeruginosa*
0.125	9	9	9	9	8	9	7
0.25	10	10	10	11	9	11	8
0.375	11	11	12	12	11	12	8
0.5	13	12	13	19	12	14	8
1	14	13	16	22	14	15	9
1.5	17	14	20	24	15	18	10
Conc. of MeOH extract of *R. graveolens* (mg/ml)	**Inhibition zone (mm)**						
	K. pneumoniae	*E. coli*	*E. clocae*	*S. aureus*	*S. epidermidis*	*Shigella* sp	*P. aeruginosa*
2.5	12	12	13	16	11	10	17
5	13	13	15	18	12	11	19
7.5	14	15	16	19	12	11	19
10	15	16	16	21	12	12	20

Table 2. The synergistic antimicrobial effect of different concentrations of AgNPs combined with 2.5 mg/ml concentration of *Ruta graveolens* MetOH extract against the different tested bacterial species.

Conc. of AgNPs (mg/ml)	Conc. of MeOH extract of *R. graveolens* (mg/ml)	*K. pneumoniae*		*E. coli*		*E. clocae*		*S. aureus*		*S. epidermidis*		*Shigella* sp		*P. aeruginosa*	
		IZ*	IFA	IZ	IFA	IZ	IFA	IZ	IFA	IZ	IFA	IZ	IFA	IZ	IFA
0.125	**2.5**	14	0.36	14	0.36	15	0.33	17	0.13	12	0.19	11	0.21	19	0.25
0.25	**2.5**	15	0.33	15	0.33	17	0.28	19	0.11	15	0.56	12	0.19	21	0.22
0.375	**2.5**	16	0.31	16	0.14	17	0.13	20	0.11	17	1.0	15	0.86	22	0.72
0.5	**2.5**	16	0.14	17	0.13	17	0.13	22	0.10	18	1.25	15	0.56	22	0.21

*IZ: inhibition zone

Minimum inhibitory concentration (MIC)

The results of minimum inhibitory concentration (MIC) showed that *R. graveolens* MetOH extract and AgNPs have antibacterial activity against *E. coli, E. cloacae, Shigella sp., Pseudomonas aeruginosa, S. epidermidis, S.aureus*, and *K.pneumoniae* with MIC values ranging from 0.5 to 2.5 mg/ml, and from 0.025 to > 0.125 mg/ml, respectively. The materials showed different levels of antimicrobial activity depending on the tested species as shown in **Table 3**. All of the bacterial strains responded to both *R. graveolens* MetOH extract and AgNPs with the same trend.

Table 3. Minimum inhibition zone of different bacterial strains caused by *R. graveolens* MetOH extract and AgNPs.

Bacteria name	MIC by *R. graveolens* MetOH extract (mg/ml)	MIC by AgNPs (mg/ml)
E. coli	2.5	0.075
E. cloacae	1	0.025
Shigella sp.	2	0.075
P. aeruginosa	2.5	> 0.125
S. epidermidis	1.5	0.05
S. aureus	2.5	0.10
K. pneumoniae	0.5	0.025

Chemical composition of R. graveolens using LC-MS

Utilizing LCMS, the active components found in the *R. graveolens* methanolic aerial parts extract were identified. **Table 4** provides a summary of the *R. graveolens* extract's general chemical profiles, percentage contents of the various components, retention indices, molecular formula, molecular weight, and chemical class distribution of the crude extract constituents. Rutin, which makes up 13.7% of the 25 components listed in **Table 4**, is the main component in *R. graveolens*. In the methanolic extract of *R. graveolens*, quercetin ranks second in abundance with a 9.3% concentration, followed by isoquinoline with a 6.9% concentration, methoxy-psoralen with a 6.8% concentration, and procyanidin with a 6.3% concentration. Other constituents were present in varying amounts, as shown in the table. These findings imply the presence of possible chemicals in *R. graveolens* extract that may aid in the chemotherapeutic or adjuvant treatment of various illnesses.

Table 4. *R. graveolens* methanolic extract's chemical components as determined using LC-MS/MS.

No	Chemical Compound	Molecular formula	Molecular weight	Retention indices R.T	%
1.	Catechin	$C_{15}H_{14}O_6$	290.27	25.31	1.4
2.	Ellagic acid	$C_{14}H_6O_8$	302.19	25.67	1.3
3.	Quercetin	$C_{15}H_{10}O_7$	302.24	25.79	9.3
4.	Coumarins	$C_{19}H_{16}O_4$	308.33	26.21	1.05
5.	Linamarin	$C_{10}H_{17}NO_6$	247.24	20.80	3.1
6.	Morphine	$C_{17}H_{19}NO_3$	285.34	24.91	3.7
7.	2-undecanone	$C_{11}H_{22}O$	170.29	11.85	1.3
8.	2-methyl-undecanal	$C_{12}H_{24}O$	184.32	13.58	1.4
9.	2-dodecanone	$C_{12}H_{24}O$	184.32	13.60	4.7
10.	2-nonanol	$C_9H_{20}O$	144.25	9.42	1.3
11.	Cis-Piperitenone epoxide	$C_{10}H_{14}O_2$	166.22	10.92	1.4
12.	Psoralen	$C_{11}H_6O_3$	186.16	13.86	4.7
13.	Angelicin	$C_{11}H_6O_3$	186.16	13.89	4.2
14.	2-Heptanol acetate	$C_9H_{16}Br_2O_2$	316.03	26.97	1.4
15.	Procyanidin	$C_{30}H_{26}O_{13}$	594.52	30.91	6.3
16.	Rutin	$C_{27}H_{30}O_{16}$	610.52	31.00	13.7
17.	Digoxin	$C_{41}H_{64}O_{14}$	780.94	31.60	1.1
18.	1-dodecanol	$C_{12}H_{26}O$	186.33	14.10	1.2
19.	Acridone	$C_{13}H_9NO$	195.22	15.90	4.7
20.	Flavan	$C_{15}H_{14}O$	210.27	18.92	3.2
21.	Methoxypsoralen	$C_{12}H_8O_4$	216.19	20.15	6.8
22.	Pyrrolizidine	C7H13N	111.18	6.12	3.5
23.	Indole	C_8H_7N	117.15	7.17	4.2
24.	Tropane	$C_8H_{15}N$	125.21	7.87	5.5
25.	Isoquinoline	C_9H_7N	129.16	8.12	6.9

Specialized Jordanian medicinal plants from the Mediterranean region exhibit several types of adaptation through the development of bioactive components [24]. *R. graveolens* is one of the most important plants used in Jordanian traditional medicine due to its medicinal, pharmacological, and curative characteristics [25]. One of the leading causes of death in the healthcare industry is infectious diseases, which are also on the rise. Despite the abundance of medications on the market, recently found multidrug-resistant (MDR) bacteria render them ineffective against them, necessitating the development of new treatments, which takes time, money, and effort. Because of the excessive use of antibiotics, MDR bacteria have developed, and their growth and spread are extremely important. Due to treatments for antimicrobial resistance based on nanotechnology, clinicians and patients now have the opportunity to address the issue of rising drug resistance [26]. Microorganisms, particularly fungi, produce silver nanoparticles more cheaply, effectively, and securely than chemical and physical processes [27]. Several commercially available antibiotic discs have previously been discovered to work effectively with a variety of plant extracts,

and the potential introduction of novel treatment modalities has promoted the success of these partnerships [19, 20].

Primary diagnostic techniques revealed that 24 hours after adding AgNO3, the fungal filtrate's dark brown color began to develop. The extracellular release of multiple fungal enzymes and the ease with which they retained their efficacy allowed them to create silver nanoparticles in vitro [28]. Nanoparticles' TEM image shows that they are spherical and range in size from 5 to 35 nm. AgNP is produced by fungi, however, the specific mechanism is yet unclear. Significant peaks were visible in the ATR-FTIR spectra at 1011, 1375, 1437, 1516, 1623, and 2401 cm-1 as well as a somewhat flat peak at about 3228 cm-1. The vibrational resonant frequency of hydrogen-containing bonds like C-H, O-H, and N-H is what causes the large peak between 3228 cm-1 and 2827 cm-1. The considerable absorption intensity values at the peaks at 1623, 1516, and 1081 cm-1 show that the COO- the group is stretched both symmetrically and asymmetrically. The protein's amino and aminomethyl stretch groups had the only peaks at 1375 cm-1 in the spectrum. However, prior studies have shown that the nitrate reductases dependent NADH, which seems to be crucial components in the synthesis of AgNPs, are required for the nitrate reduction process [27].

At all concentrations of silver nanoparticles, all tested bacteria had anti-bacterial actions, and these effects grew stronger with increasing concentration. At a concentration of 0.125 mg/ml of AgNPs, *Escherichia coli, Klebsiella pneumonia, E. cloacae, Shigella sp., Pseudomonas aeruginosa, Staphylococcus aureus,* and *Staphylococcus epidermidis* were all inhibited with inhibition zones varying from 7 to 9 mm. The inhibition zones of all the bacteria ranged from 10 to 24 mm when using the maximal AgNPs concentration of 1.5 mg/mL. *R. graveolens* is one medicinal plant that has been particularly well-documented for its therapeutic benefits, which include the treatment of inflammatory disorders, eczema, ulcers, and arthritis [29]. In contrast to S. aureus, S. epidermidis cells showed sensitivity to all AgNP concentrations and MetOH extract from *R. graveolens*, both individually and in combination, according to this study. For all of the studied bacterial strains, as previously reported [30]. The combined use of *R. graveolens* MetOH extract and data clearly showed a significant reduction in the required concentration of AgNPs. Our results support research indicating that *R. graveolens* leaf extract, either alone or in combination with AgNPs, is functionally acceptable for application to animal cells and has potential use as antibacterial, insecticidal, and immunomodulatory effects [31-33].

These variations in the sensitivity of gram-positive and gram-negative bacteria to nanoparticles may result from these differences in the cell surfaces of these bacteria [22]. The activity of the AgNPs (such as antimicrobial efficacy) depends on their specific surface areas. The efficacy of nanoparticles increases with the increase of its surface area as a reason for the increase in surface energy [34]. According to their large surface areas and its highly reactive components, AgNPs are highly toxic to microorganisms [35]. Investigators have looked into the naturally occurring AgNPs derived from fungi and their antibacterial properties. When AgNPs and *R. graveolens* MetOH extract were combined, the antimicrobial efficacy against *P. aeruginosa* was enhanced. For AgNPs concentrations of 0.125, 0.25, 0.375, and 0.5 mg/ml, the IFA of the synergistic results were 0.25, 0.22, 0.72, and 0.21, respectively.

The presence of significant inhibitory zones measuring 19 to 22 mm indicated that *P. aeruginosa* was susceptible to the combination of various dosages of AgNP and 2.5 mg/mL of *R. graveolens* MetOH extract. *P. aeruginosa* was observed to be highly impacted by the synergistic activity of these two components, in contrast to other bacterial species studied *P. aeruginosa* responded to AgNPs more favorably than *E. coli*, as was previously noted [36]. These findings are in line with recent research demonstrating that the mechanisms of action of medications, when taken in combination, might occasionally differ significantly from those of the same treatments when taken separately [37]. There is an inverse relationship between the of AgNPs, their bactericidal action, and the type of bacteria. Different bacterial species react differently to AgNPs [38]. It has been demonstrated that silver nanoparticles kill S. aureus more effectively than *E. coli* and *S. epidermis*, likely due to differences in the cell walls and membranes of the bacteria [39, 40].

The results of minimum inhibitory concentration (MIC) showed that *R. graveolens* MetOH extract and AgNPs have antibacterial activity against *E. coli, E. cloacae, Shigella sp., Pseudomonas aeruginosa, S. epidermidis, S. aureus*, and *K. pneumoniae* with MIC values ranging from 0.5 to 2.5 mg/ml, and from 0.025 to > 0.125 mg/ml, respectively. All of the bacterial strains responded to both *R. graveolens* MetOH extract and AgNPs with the same trend. It was clear that *K. pneumoniae* was the most susceptible strain to both of them; meanwhile, *S. aureus* and *P. aeruginosa* were the most resistant isolates. This confirms several previous findings [33] that found that Gram-positive and Gram-negative bacteria have different susceptibilities to AgNPs. This difference is possibly due to differences in bacterial membranes and cell walls [39].

Conclusion

In conclusion, the results of the current study demonstrated that the investigated plant has different levels of antibacterial activities. The results of the inhibition zone were following the values of MICs for the tested plant extract.

The current study's findings showed that 26 components were found in *R. graveolens*' methanolic extract and that the plant under investigation has varying degrees of biological activity depending on its constituent phytochemicals. *R. graveolens* has been used to identify phytochemicals including alkaloids, coumarins, isoquinoline, terpenoids, methoxy-psoralen, volatile compounds, rutin, furoquinolines, and flavonoids. An earlier investigation into the phytochemical composition of several solvent extracts of *R. graveolens* revealed the presence of additional classes of molecules, including phenols, glycosides, phenolic compounds, and cardiac glycolipids [41]. According to

Hashemi *et al*. (2011) saponin, tannins, and glycosides are present [42]. The occurrence of several chemotypes can most likely be used to explain these chemical distinctions [41]. A fundamental to understanding the scavenging ability of phenolic compounds, which reflects their significant potential as antioxidants, antimicrobials, and antiparasitic agents, is the existence of several chemotypes containing hydroxyl groups in phenolic compounds. These substances demonstrated antioxidant, antiparasitic, and antibacterial action against several bacterial strains [41]. When the tested extract was compared to available data on the oil content of other *R. graveolens* samples, the chemical composition of the tested extract significantly changed, and several quantitative and qualitative discrepancies were revealed [42]. The occurrence of several chemotypes can most likely be used to explain these chemical distinctions [43]. Different chemotypes of phenolic compounds with hydroxyl groups are key to understanding their scavenging capacity, which reflects their significant potential as antioxidants, antimicrobials, and anti-parasitic agents [41].

Acknowledgments: The Mutah University, Deanship of Scientific Research assisted the authors in carrying out this study with decision No. 356/2020.

Conflict of interest: None

Financial support: Deanship of Scientific Research at Mutah university/Jordan supported this research with grant proposals 315/2020.

Ethics statement: Not applicable because no invivo studies involved.

References

1. Ingole AR, Thakare SR, Khati NT, Wankhade AV, Burghate DK. Green synthesis of selenium nanoparticles under ambient condition. Chalcogenide Lett. 2010;7(7):485-9.
2. Calderón-Jiménez B, Johnson ME, Montoro Bustos AR, Murphy KE, Winchester MR, Vega Baudrit JR. Silver nanoparticles: Technological advances, societal impacts, and metrological challenges. Front Chem. 2017;5:6.
3. Satalkar P, Elger BS, Shaw DM. Defining nano, nanotechnology and nanomedicine: why should it matter?. Sci Eng Ethics. 2016;22:1255-76.
4. Sergeev GB, Shabatina TI. Cryochemistry of nanometals. Colloids Surf. 2008;313:18-22.
5. Colvin VL, Schlamp MC, Alivisatos AP. Light-emitting diodes made from cadmium selenide nanocrystals and a semiconducting polymer. Nature. 1994;370(6488):354-7.
6. Xu ZP, Zeng QH, Lu GQ, Yu AB. Inorganic nanoparticles as carriers for efficient cellular delivery. Chem Eng Sci. 2006;61(3):1027-40.
7. Mafuné F, Kohno JY, Takeda Y, Kondow T, Sawabe H. Formation of gold nanoparticles by laser ablation in aqueous solution of surfactant. J Phys Chem B. 2001;105(22):5114-20.
8. Kabashin AV, Meunier M. Synthesis of colloidal nanoparticles during femtosecond laser ablation of gold in water. J Appl Phys. 2003;94(12):7941-3.
9. Sylvestre JP, Kabashin AV, Sacher E, Meunier M, Luong JH. Stabilization and size control of gold nanoparticles during laser ablation in aqueous cyclodextrins. J Am Chem Soc. 2004;126(23):7176-7.
10. Klaus T, Joerger R, Olsson E, Granqvist CG. Silver-based crystalline nanoparticles, microbially fabricated. Proc Natl Acad Sci. 1999;96(24):13611-4.
11. Gentile A, Ruffino F, Grimaldi MG. Complex-morphology metal-based nanostructures: Fabrication, characterization, and applications. Nanomaterials. 2016;6(6):110.
12. Dallas P, Sharma VK, Zboril R. Silver polymeric nanocomposites as advanced antimicrobial agents: classification, synthetic paths, applications, and perspectives. Adv Colloid Interface Sci. 2011;166(1-2):119-35.
13. Al-Soub A, Khleifat K, Al-Tarawneh A, Al-Limoun M, Alfarrayeh I, Al Sarayreh A, et al. Silver nanoparticles biosynthesis using an airborne fungal isolate, Aspergillus flavus: optimization, characterization and antibacterial activity. Iran J Microbiol. 2022;14(4).
14. Wayne PA. Clinical and Laboratory Standards Institute: Performance standards for antimicrobial susceptibility testing: 20th informational supplement. CLSI document M100-S20. 2010.
15. Khleifat K, Abboud MM. Correlation between bacterial haemoglobin gene (vgb) and aeration: their effect on the growth and α-amylase activity in transformed Enterobacter aerogenes. J Appl Microbiol. 2003;94(6):1052-8.
16. Khleifat KM, Abboud MM, Omar S, Al-Kurishy JH. Urinary tract infection in South Jordanian population. J Med Sci. 2006;6(1):5-11.
17. Khleifat KM, Sharaf EF, Al-limoun MO. Biodegradation of 2-chlorobenzoic acid by enterobacter cloacae: Growth kinetics and effect of growth conditions. Bioremediat J. 2015;19(3):207-17.
18. Qaralleh H, Khleifat KM, Al-Limoun MO, Alzedaneen FY, Al-Tawarah N. Antibacterial and synergistic effect of biosynthesized silver nanoparticles using the fungi Tritirachium oryzae W5H with essential oil of Centaurea damascena to enhance conventional antibiotics activity. Adv Nat Sci: Nanosci Nanotechnol. 2019;10(2):025016.
19. Khleifat KM, Matar SA, Jaafreh M, Qaralleh H, Al-limoun MO, Alsharafa KY. Essential oil of Centaurea damascena aerial parts, antibacterial and synergistic effect. J Essent Oil Bear Plants. 2019;22(2):356-67.
20. Al-Tawarah NM, Qaralleh H, Khlaifat AM, Nofal MN, Alqaraleh M, Khleifat KM, et al. Anticancer and antibacterial properties of verthemia iphionides essential oil/silver nanoparticles. Biomed Pharmacol J. 2020;13(3):1175-85.

21. Khleifat KM, Tarawneh KA, Ali Wedyan M, Al-Tarawneh AA, Al Sharafa K. Growth kinetics and toxicity of Enterobacter cloacae grown on linear alkylbenzene sulfonate as sole carbon source. Curr Microbiol. 2008;57:364-70.
22. Joanna C, Marcin L, Ewa K, Gražyna P. A nonspecific synergistic effect of biogenic silver nanoparticles and biosurfactant towards environmental bacteria and fungi. Ecotoxicology. 2018;27:352-9.
23. Pérez-Nava J, Hernández-Aldana F, Martínez-Valenzuela C, Rivera A. Pseudomonas sp Isolated from Wastewater and their Interaction with Microalgae. J Biochem Technol. 2021;12(2):1-5.
24. Carvalho LS, Queiroz LS, Alves Junior IJ, Almeida AD, Coimbra ES, de Faria Pinto P, et al. In vitro schistosomicidal activity of the alkaloid-rich fraction from Ruta graveolens L.(Rutaceae) and its characterization by UPLC-QTOF-MS. Evid-Based Complementary Altern Med. 2019;2019.
25. Oran SA, Al-Eisawi DM. Check-list of medicinal plants in Jordan. Dirasat. 1998;25(2):84-112.
26. Mubeen B, Ansar AN, Rasool R, Ullah I, Imam SS, Alshehri S, et al. Nanotechnology as a novel approach in combating microbes providing an alternative to antibiotics. Antibiotics. 2021;10(12):1473.
27. Khlaifat AM, Al-limoun MO, Khleifat KM, Al Tarawneh AA, Qaralleh H, Rayyan EA, et al. Antibacterial synergy of Tritirachium oryzae-produced silver nanoparticles with different antibiotics and essential oils derived from Cupressus sempervirens and Asteriscus graveolens (Forssk). Trop J Pharm Res. 2019;18(12):2605-16.
28. Al-Limoun M, Qaralleh HN, Khleifat KM, Al-Anber M, Al-Tarawneh A, Al-sharafa K, et al. Culture media composition and reduction potential optimization of mycelia-free filtrate for the biosynthesis of silver nanoparticles using the fungus Tritirachium oryzae W5H. Curr Nanosci. 2020;16(5):757-69.
29. Fadlalla K, Watson A, Yehualaeshet T, Turner T, Samuel T. Ruta graveolens extract induces DNA damage pathways and blocks Akt activation to inhibit cancer cell proliferation and survival. Anticancer Res. 2011;31(1):233-41.
30. Saravanan M, Arokiyaraj S, Lakshmi T, Pugazhendhi A. Synthesis of silver nanoparticles from Phenerochaete chrysosporium (MTCC-787) and their antibacterial activity against human pathogenic bacteria. Microb Pathog. 2018;117:68-72.
31. Gurunathan S, Kalishwaralal K, Vaidyanathan R, Venkataraman D, Pandian SR, Muniyandi J, et al. Biosynthesis, purification and characterization of silver nanoparticles using Escherichia coli. Colloids Surf B. 2009;74(1):328-35.
32. Ghramh HA, Ibrahim EH, Kilnay M, Ahmad Z, Alhag SK, Khan KA, et al. Silver nanoparticle production by Ruta graveolens and testing its safety, bioactivity, immune modulation, anticancer, and insecticidal potentials. Bioinorg Chem Appl. 2020;2020.
33. Khleifat K, Qaralleh H, Al-Limoun M. Antibacterial Activity of Silver Nanoparticles Synthesized by Aspergillus flavusand its Synergistic Effect with Antibiotics. J Pure Appl Microbiol. 2022.
34. Jiang J, Oberdörster G, Biswas P. Characterization of size, surface charge, and agglomeration state of nanoparticle dispersions for toxicological studies. J Nanopart Res. 2009;11:77-89.
35. Ghosh S, Patil S, Ahire M, Kitture R, Kale S, Pardesi K, et al. Synthesis of silver nanoparticles using Dioscorea bulbifera tuber extract and evaluation of its synergistic potential in combination with antimicrobial agents. Int J Nanomed. 2012:483-96.
36. Zhang X, Yan S, Tyagi RD, Surampalli RY. Synthesis of nanoparticles by microorganisms and their application in enhancing microbiological reaction rates. Chemosphere. 2011;82(4):489-94.
37. Khlaifat AM, Al-limoun MO, Khleifat KM, Al Tarawneh AA, Qaralleh H, Rayyan EA, et al. Antibacterial synergy of Tritirachium oryzae-produced silver nanoparticles with different antibiotics and essential oils derived from Cupressus sempervirens and Asteriscus graveolens (Forssk). Trop J Pharm Res. 2019;18(12):2605-16.
38. Rahimi G, Alizadeh F, Khodavandi A. Mycosynthesis of silver nanoparticles from Candida albicans and its antibacterial activity against Escherichia coli and Staphylococcus aureus. Trop J Pharm Res. 2016;15(2):371-5.
39. Feng QL, Wu J, Chen GQ, Cui FZ, Kim TN, Kim JO. A mechanistic study of the antibacterial effect of silver ions on Escherichia coli and Staphylococcus aureus. J Biomed Mater Res. 2000;52(4):662-8.
40. Singh T, Jyoti K, Patnaik A, Singh A, Chauhan R, Chandel SS. Biosynthesis, characterization and antibacterial activity of silver nanoparticles using an endophytic fungal supernatant of Raphanus sativus. J Genet Eng Biotechnol. 2017;15(1):31-9.
41. Amabye TG, Shalkh TM. Phytochemical screening and evaluation of the antibacterial activity of R. graveolens L.—A medicinal plant grown around Mekelle, Tigray, Ethiopia. Nat Prod Chem Res. 2015;3:195. doi:10.4172/2329-6836.1000195
42. Hashemi KS, Sadeghpour HM, Gholampour AI, Mirzaei JH. Survey the antifungal effect of root ethanol extract of Ruta graveolens on Saprolegnia spp. In Int Conf Biotechnol Environ Manag 2011 (Vol. 18, pp. 19-23).
43. Kostova I, Ivanova A, Mikhova B, Klaiber I. Alkaloide und cumarine aus Ruta graveolens. Monatsh Chem/Chem Mthly. 1999;130(5):703-7.